UNIVERSITY OF WEST BOHEMIA

Applied and Computational Mechanics 1 (2007) 417 - 426

Applied and Computational Mechanics

A nonlinear truss finite element with varying stiffness

R. Ďuriš [a,*], J. Murín [b]

[a] *Department of Applied Mechanics, Faculty of Materials Science and Technology in Trnava, Slovak University of Technology in Bratislava, Paulínska 16, 917 24 Trnava, Slovak Republic*

[b] *Department of Mechanics, Faculty of Electrical Engineering and Information Technology, Slovak University of Technology, Ilkovičova 3, 812 19 Bratislava, Slovak Republic*

Received 10 September 2007; received in revised form 9 October 2007

Abstract

This contribution deals with a new truss element with varying stiffness intended to geometric and physically nonlinear analysis of composite structures. We present a two-node straight composite truss finite element derived by new nonincremental full geometric nonlinear approach. Stiffness matrix of this composite truss contains transfer constants, which accurately describe the polynomial longitudinal variation of cross-section area and material properties. These variations could be caused by nonhomogenous temperature field or by varying components volume fractions of the composite or/and functionally graded materials (FGM´s). Numerical examples were solved to verify the established relations. The accuracy of the new proposed finite truss element are compared and discused.

Keywords: geometric nonlinearity, plasticity, truss finite element, varying stiffness, functionally graded material

1. Introduction

The composite structures (e.g. laminate, sandwich structures, or FGM´s) are often used in many applications. Their FE analyses require creating very fine mesh of elements even for relatively small sized bodies, what increases computational time, particularly in nonlinear analyses. Usually, the analysis of composite bar structures can be performed using the truss or beam elements with constant „average" cross-sectional area and Young modulus. Sufficient accuracy can achieved by increasing the number of integration points in the assembled stiffness matrix, with refining the mesh, and by choosing of elements with higher order interpolation polynomials. In addition, the linearisation of the nonlinear expressions is the reason for increasing solution inaccuracy. The main aim of this paper is to present new more effective truss element with continuous variation of the stiffness along its axis suitable for the solution of geometric and physical nonlinear problems. The nonincremental nonlinearised Lagrangian formulation of the nonlinear FEM-equations will be used to avoid inaccuracy caused by the linearisation of the Green-Lagrange strain tensor increment. A new shape functions of a truss element [3,4] have been used to overcome the problems associated with using an inaccurate description of stiffness variation along the element length.

2. Basic equations

2.1. New shape functions for a truss element with varying stiffness

To avoid element size influence on the accuracy of the results, we will first describe new shape functions for the truss element with varying stiffness and then we will use these shape functions for the expresion of the axial displacement in stiffness matrix derivation of the non-

* Corresponding author. Tel.: +420 33 55 11 601, e-mail: rastislav.duris@stuba.sk.

linear truss element satisfying equilibrium conditions both locally and globally. It can be assumed that the variation of the parameters defining the cross-section area $A(x)$ can be then expressed in following polynomial form

$$A(x) = A_i\left(1 + \sum_{k=1}^{p} \eta_{Ak} x^k\right) = A_i\, \eta_A(x) \ . \tag{1}$$

Young modulus $E(x)$ is defined similarly

$$E(x) = E_i\left(1 + \sum_{k=1}^{q} \eta_{Ek} x^k\right) = E_i\, \eta_E(x) \ . \tag{2}$$

In eqs. (1) and (2) subscript i denotes the variables value at node i of the element (see Fig. 1). The polynomials $\eta(x)$ are defined as follows: the polynomial for the variation of cross-sectional area and the Young modulus are $\eta_A(x) = A(x)/A_i$ and $\eta_E(x) = E(x)/E_i$, where A_i and E_i are their values at node i. $\sigma_y(x)$ and $E_T(x)$ is the yield stress and elastoplastic modulus, defined by a similar way as below. Then the variation of axial elastic stiffness can be written as

$$A(x)\,E(x) = A_i\, E_i\, \eta_E(x)\, \eta_A(x) = A_i\, E_i\, \eta_{AE}(x) \ . \tag{3}$$

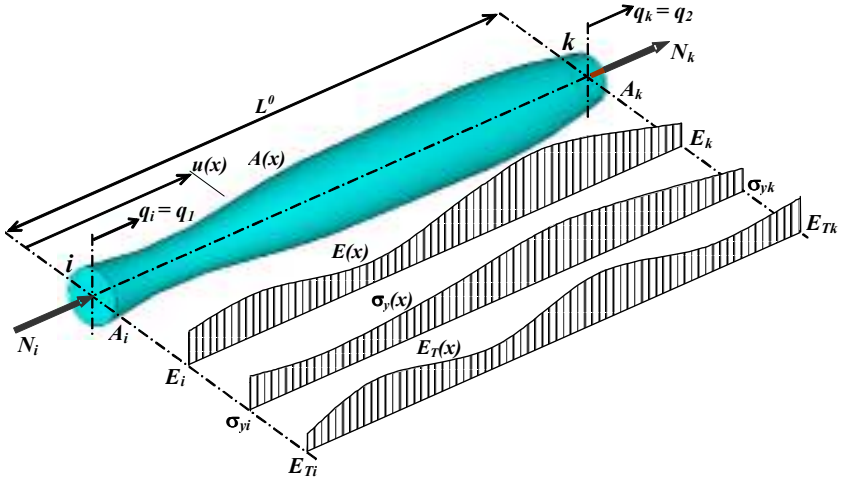

Fig. 1. Two node truss element with variation of geometry and material properties in the initial state.

2.2. *Shape functions for axial displacement*

The elastic kinematical relation between first derivative of the axial displacement function $u(x)$ and axial force $N(x)$ at x is

$$u'(x) = \frac{N(x)}{A(x)\,E(x)} = \frac{N(x)}{A_i\, E_i\, \eta_{AE}(x)} \ . \tag{4}$$

If we define the second derivative of the transfer function $d_{2e}(x)$ for pure tension-compression as

$$d''_{2e}(x) = \frac{1}{\eta_{AE}(x)} \ , \tag{5}$$

then the solution of the differential equation (4), assuming that all element loads are transferred to the nodal points and axial force is constant ($N(x) = N_i$), is a function of axial displacement

$$u(x) = q_i - \frac{N_i}{A_i E_i} d'_{2e}(x) \ . \tag{6}$$

By replacing $x = L^0$ in eq. (6), displacement $u(L^0) = q_k$ and $d'_{2e}(L^0) = d'_{2e}$ is the value of the first derivative of the transfer function, which is also called a transfer constant for pure tension-compression. Deriving the axial force N_i from this equation and by its back substitution in-

to eq. (6) the expression relating the axial displacement of an arbitrary point x and the axial displacements of nodal points i and k becomes,

$$u(x) = \left(1 - \frac{d'_{2e}(x)}{d'_{2e}}\right) q_i + \frac{d'_{2e}(x)}{d'_{2e}} q_k = \phi_{ui}(x)\, q_i + \phi_{uk}(x)\, q_k \ . \tag{7}$$

Then, the shape functions of the first ($i = 1$) and second ($k = 2$) nodal points for two node truss element (first index $u = 1$ determines the local displacement direction) are defined as

$$\phi_{ui}(x) = \phi_{11}(x) = 1 - \frac{d'_{2e}(x)}{d'_{2e}} \quad , \quad \phi_{uk}(x) = \phi_{12}(x) = \frac{d'_{2e}(x)}{d'_{2e}} \ . \tag{8}$$

The evaluation of the transfer constants for tension-compression is performed using a simple numerical algorithm published in [1,2,3]. For a constant stiffness, $d'_{2e}(x) = x$ and $d'_{2e} = L^0$ and eq. (7) leads to the standard shape functions for the truss element. The first derivatives required for the stiffness matrices (see later eqs. 14-17) are

$$\phi_{11,1}(x) = -\frac{d''_{2e}(x)}{d'_{2e}} \quad , \quad \phi_{12,1}(x) = \frac{d''_{2e}(x)}{d'_{2e}} \ . \tag{9}$$

2.3. Nonincremental geometric nonlinear FEM equations without linearisation

With the objective to minimize negative influence of commonly used linearisation of incremental equations to derive stiffness matrices we will use a new nonincremental formulation without any linearisation [1,4]. From the principle of virtual work,

$$\int_{V^0} S_{ij}\, \delta E_{ij}\, dV = \int_{A^0} F_i\, \delta u_i\, dA + \vec{F}_k\, \delta q_k \tag{10a}$$

the general nonlinear equation can be derived in the current configuration in nonincremental form as

$$\int_{V^0} C_{ijkl}\, e_{kl}\, \delta e_{ij}\, dV + \int_{V^0} C_{ijkl}(\eta_{kl}\, \delta e_{ij} + e_{kl}\, \delta \eta_{ij} + \eta_{kl}\, \delta \eta_{ij}) dV = \int_{A^0} F_i\, \delta u_i\, dA + \vec{F}_k\, \delta q_k \ , \tag{10b}$$

where C_{ijkl} is a tensor of material properties defining constitutive relation of second Piola-Kirchhoff stress tensor S_{ij} and Green-Lagrange deformation tensor $E_{ij} = e_{ij} + \eta_{ij}$, where $e_{ij} = \frac{1}{2}(u_{i,j} + u_{j,i})$ and $\eta_{ij} = \frac{1}{2} u_{k,i}\, u_{k,j}$ is its linear and nonlinear part, respectively. Further, $u_{i,j}$ is the current displacement gradient, F_i are the surface tractions (δu_i is the variation of displacement field), and δq_k are virtual displacements of points of application of $\vec{F}_k$. Integration is performed through the initial (undeformed) volume V^0 and initial area A^0 of a finite element. Let the unknown displacement field of the element be $u_i = \phi_{ik}\, q_k$, where ϕ_{ik} are the shape functions and q_k are the nodal displacement components. By substituting these relations into eq. (10b) and after necessary modifications, we obtain the following equation

$$\begin{aligned} &\frac{1}{4} \int_{V^0} C_{ijkl}(\phi_{km,l} + \phi_{lm,k})(\phi_{in,j} + \phi_{jn,i}) q_m\, dV + \frac{1}{4} \int_{V^0} C_{ijkl}\, \phi_{pm,k}\, \phi_{pr,l}(\phi_{in,j} + \phi_{jn,i}) q_m\, q_r\, dV + \\ &\frac{1}{2} \int_{V^0} C_{ijkl}\, \phi_{pr,i}\, \phi_{pn,j}(\phi_{km,l} + \phi_{lm,k}) q_m\, q_r\, dV + \frac{1}{2} \int_{V^0} C_{ijkl}\, \phi_{pm,k}\, \phi_{pv,l}\, \phi_{rq,i}\, \phi_{rn,j}\, q_m\, q_v\, q_q\, dV \\ &= \int_{A^0} F_i\, \phi_{in}\, dA + \vec{F}_n \ . \end{aligned} \tag{11}$$

Equation (11) can be rewritten in a simpler form $K_{nm}\, q_m = F_n$ or in matrix notation

$$\mathbf{K}(\mathbf{q})\, \mathbf{q} = \mathbf{F} \ , \tag{12}$$

where K_{nm} are the components of local nonlinear stiffness matrix $\mathbf{K}(\mathbf{q})$, q_m are the components of nodal displacement vector $\mathbf{q}$, and F_n are the components of external loading vector $\mathbf{F}$ at nodal

points. The local nonlinear stiffness matrix consists of one linear and three nonlinear parts

$$\mathbf{K}(\mathbf{q}) = \mathbf{K}^{L} + \mathbf{K}^{NL1}(q) + \mathbf{K}^{NL2}(q) + \mathbf{K}^{NL3}(q) = \mathbf{K}^{L} + \mathbf{K}^{NL}(\mathbf{q}) \ . \tag{13}$$

The components of linear stiffness matrix $\mathbf{K}^{L}$ can be derived from the first integral of eq. (11)

$$K^{L}_{nm} = \frac{1}{4}\int_{V^0} C_{ijkl}(\phi_{km,l} + \phi_{lm,k})(\phi_{in,j} + \phi_{jn,i})dV \ . \tag{14}$$

Equation (14) corresponds to the classical linear stiffness matrix from the linear FEM theory. The three nonlinear stiffness matrices $\mathbf{K}^{NL1}$, $\mathbf{K}^{NL2}$ and $\mathbf{K}^{NL3}$ contains following components

$$K^{NL1}_{nm} = \frac{1}{4}\int_{V^0} C_{ijkl}\,\phi_{pm,k}\,\phi_{pr,l}(\phi_{in,j} + \phi_{jn,i})\,q_r\,dV \ , \tag{15}$$

$$K^{NL2}_{nm} = \frac{1}{2}\int_{V^0} C_{ijkl}\,\phi_{pr,i}\,\phi_{pn,j}(\phi_{km,l} + \phi_{lm,k})\,q_r\,dV \ , \tag{16}$$

$$K^{NL3}_{nm} = \frac{1}{2}\int_{V^0} C_{ijkl}\,\phi_{pm,k}\,\phi_{pv,l}\,\phi_{rq,i}\,\phi_{rn,j}\,q_v\,q_q\,dV \ . \tag{17}$$

The nonlinear system of equations is solved by an iterative method. To ensure the quadratic convergence of the solution (e.g. in the Newton-Rhapson iteration scheme), the tangent stiffness matrix for the element needs to be assembled according to the expression

$$\mathbf{K}_T(\mathbf{q}) = \frac{\partial \mathbf{F}}{\partial \mathbf{q}} = \mathbf{K}(\mathbf{q}) + \frac{\partial \mathbf{K}(\mathbf{q})}{\partial \mathbf{q}}\mathbf{q} = \mathbf{K}^{L} + \mathbf{K}^{NLT}(\mathbf{q}) \ , \tag{18}$$

where $\mathbf{K}^{NLT}(\mathbf{q})$ is the nonlinear part of tangent stiffness matrix $\mathbf{K}_T(\mathbf{q})$ [5].

2.4. Geometrically nonlinear local stiffness matrix of the truss element for linear elastic analysis

Substituting (9) into eqs. (14-17) and for $dV = A(x)\,dx = A_i\eta_A(x)dx$, where the tensor of elasticity is $C_{ijkl} \equiv E(x)$, we obtain linear and three nonlinear stiffness matrices of the truss element. For the local coordinate system of the truss element the free indices m, n are 1 and 2, respectively. The linear stiffness matrix of the truss element with varying stiffness has the form

$$\mathbf{K}^{L} = \frac{A_i E_i}{d'_{2e}}\begin{bmatrix} 1 & -1 \\ -1 & 1 \end{bmatrix} . \tag{19}$$

The first, second and third nonlinear stiffness matrices have then the form of

$$\mathbf{K}^{NL1}(q) = \frac{1}{2}\frac{A_i E_i}{(d'_{2e})^3}\begin{bmatrix} 1 & -1 \\ -1 & 1 \end{bmatrix}(q_2 - q_1)\overline{d_{2e}} \ , \tag{20}$$

$$\mathbf{K}^{NL2}(q) = \frac{A_i E_i}{(d'_{2e})^3}\begin{bmatrix} 1 & -1 \\ -1 & 1 \end{bmatrix}(q_2 - q_1)\overline{d_{2e}} \ , \tag{21}$$

$$\mathbf{K}^{NL3}(q) = \frac{1}{2}\frac{A_i E_i}{(d'_{2e})^4}\begin{bmatrix} 1 & -1 \\ -1 & 1 \end{bmatrix}(q_2 - q_1)^2\overline{\overline{d_{2e}}} \ . \tag{22}$$

Equations (15) and (16) leads to the integral $\int_{L^0}(d''_{2e}(x))^2 dx$. Expression (17) contains the integral $\int_{L^0}(d''_{2e}(x))^3 dx$. Substituting the integrant by eq. (5) and rewriting $(\eta_{AE}(x))^2 = \overline{\eta}_{AE}(x)$ and $(\eta_{AE}(x))^3 = \overline{\overline{\eta}}_{AE}(x)$ yields $\int_{L^0}(d''_{2e}(x))^2 dx = \overline{d_{2e}}$ and $\int_{L^0}(d''_{2e}(x))^3 dx = \overline{\overline{d_{2e}}}$. These are the new transfer constants of the truss element, since $\overline{\eta}_{EA}(x)$ and $\overline{\overline{\eta}}_{EA}(x)$ are again polynomials. These transfer con-

stants can be computed by using simple numerical algorithm mentioned above. The final local nonlinear stiffness matrix of the truss element, with varying stiffness, can be then written in the form

$$\mathbf{K}(\mathbf{q}) = (k_e^L + k_e^{NL})\begin{bmatrix} 1 & -1 \\ -1 & 1 \end{bmatrix} = k_e^L\left[1 + \frac{3}{2}(q_2 - q_1)\frac{\overline{d_{2e}}}{(d'_{2e})^2} + \frac{1}{2}(q_2 - q_1)^2\frac{\overline{\overline{d_{2e}}}}{(d'_{2e})^3}\right]\begin{bmatrix} 1 & -1 \\ -1 & 1 \end{bmatrix}, \quad (23)$$

where the linear part of truss element stiffness is

$$k_e^L = \frac{A_i E_i}{d'_{2e}}. \quad (24)$$

The matrix form of the local equation of equilibrium is then given by eq. (12), where $\mathbf{K}(\mathbf{q})$ is defined by (11), the vector of nodal displacements is $\mathbf{q} = [q_1 \quad q_2]^{\mathrm{T}}$ and $\mathbf{F}$ is the vector of external local nodal forces.

2.5. Local nonlinear tangent stiffness matrix

The tangent stiffness matrix is defined by eq. (18) where the matrix $\mathbf{K}(\mathbf{q})$ is defined by expression (23). After the indicated differentiation, we obtain the tangent stiffness matrix of the truss element, with varying stiffness, in the form

$$\mathbf{K}_T(\mathbf{q}) = (k_e^L + k_e^{NLT})\begin{bmatrix} 1 & -1 \\ -1 & 1 \end{bmatrix}, \quad (25)$$

where the nonlinear tangent stiffness k_e^{NLT} is expressed as the following

$$k_e^{NLT} = k_e^L\left[3(q_2 - q_1)\frac{\overline{d_{2e}}}{(d'_{2e})^2} + \frac{3}{2}(q_2 - q_1)^2\frac{\overline{\overline{d_{2e}}}}{(d'_{2e})^3}\right]. \quad (26)$$

2.6. Global nonlinear stiffness matrix

Since the local nonlinear tangent stiffness matrix (25) is not invariant to rigid body motion, it is not possible to use the conventional transformation, known from the linear theory. If the local displacements are substituted with the invariant stretching

$$\lambda = \frac{L}{L^0} = 1 + \frac{\Delta L}{L^0} = 1 + \frac{q_2 - q_1}{L^0} \quad (27)$$

we obtain the invariant nonlinear tangent stiffness in the form

$$k_e^{NLT} = k_e^L\left[3(\lambda - 1)L^0\frac{\overline{d_{2e}}}{(d'_{2e})^2} + \frac{3}{2}(\lambda - 1)^2(L^0)^2\frac{\overline{\overline{d_{2e}}}}{(d'_{2e})^3}\right]. \quad (28)$$

Using invariant nonlinear tangent stiffness (28) in the local tangent stiffness matrix (25), the global nonlinear tangent stiffness matrix $\mathbf{K}_T^G$ can be expressed in classical form as $\mathbf{K}_T^G = \mathbf{T}^{\mathrm{T}}\,\mathbf{K}_T(\mathbf{q})\,\mathbf{T}$. Matrix $\mathbf{T}$ is transformation matrix for the truss in plane and has the form

$$\mathbf{T} = \begin{bmatrix} \cos\alpha & \sin\alpha & 0 & 0 \\ 0 & 0 & \cos\alpha & \sin\alpha \end{bmatrix}, \quad (29)$$

where α is the angle determining the location of local axis in current configuration (current nodal coordinates and current truss length L), i.e. $\cos\alpha = (x_k - x_i)/L$ and $\sin\alpha = (y_k - y_i)/L$.

2.7. Internal forces

To overcome problems with transformation of internal forces from local to global coordinate system, we rewrite nonlinear stiffness matrix (23) using stretching parameter (27) to the form

$$\mathbf{K}(\mathbf{q}) = \frac{A_i E_i}{d'_{2e}}\left[1+\frac{3}{2}(\lambda-1)L^0\frac{\overline{d_{2e}}}{(d'_{2e})^2}+\frac{1}{2}(\lambda-1)^2(L^0)^2\frac{\overline{\overline{d_{2e}}}}{(d'_{2e})^3}\right]\begin{bmatrix}1 & -1\\ -1 & 1\end{bmatrix} = k_e\begin{bmatrix}1 & -1\\ -1 & 1\end{bmatrix}. \quad (30)$$

where $k_e = k_e^L + k_e^{NL}$. Then local internal axial forces can be calculated by

$$N_i = -\left[k_e^L + k_e^{NL}\right](\lambda-1)L^0 = -N_k \ . \quad (31)$$

Using invariant stretching the previous equation can be rewritten into

$$N_i = -\frac{A_i E_i}{d'_{2e}}\left[1+\frac{3}{2}(\lambda-1)L^0\frac{\overline{d_{2e}}}{(d'_{2e})^2}+\frac{1}{2}(\lambda-1)^2(L^0)^2\frac{\overline{\overline{d_{2e}}}}{(d'_{2e})^3}\right](\lambda-1)L^0 . \quad (32)$$

In the solution process the vector of global internal forces has to be calculated. Global internal forces are calculated through the internal axial force (32) and transformation matrix **T** .

2.8. Nonincremental FEM equations for geometric and physically nonlinear analysis

In this contribution only bilinear stress-strain relation is considered (Fig. 2) with isotropic and kinematic hardening. In the following derivation we use decomposition of axial strain $\varepsilon = \varepsilon_{\sigma y} + \varepsilon_{ep}$ due to nonincremental solution. If another constitutive law of stress-strain relationship or cyclic loading will be considered, incremental formulation and traditional decomposition of strain $\varepsilon = \varepsilon_e + \varepsilon_p$ and plastic modulus $H(x)$ are needed.

The cross-sectional area $A(x)$ and elasticity modulus $E(x)$ are defined using eqs. (1) and (2). The elastoplasticity modulus $E_T(x)$ is defined by similar expresion

$$E_T(x) = E_{Ti}\left(1+\sum_{k=1}^{r}\eta_{E_T k}x^k\right) \ . \quad (33)$$

Then the variation of axial elastoplastic stiffness can be written as

$$A(x)E_T(x) = A_i E_{Ti}\,\eta_A(x)\eta_{E_T}(x) = A_i E_{Ti}\,\eta_{AE_T}(x) \ . \quad (34)$$

If the axial stress exceeds the yield stress σ_y, it is neccesary to establish new relationship between the stress increment and the strain in the bar.

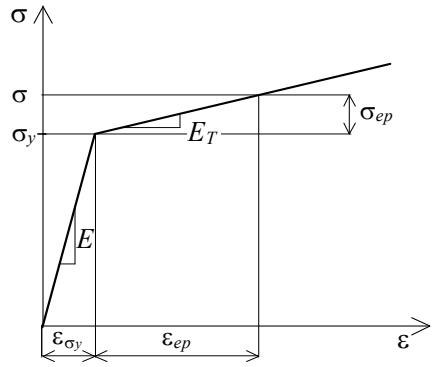

Fig. 2. One-dimensional bilinear stress-strain relationship with hardening.

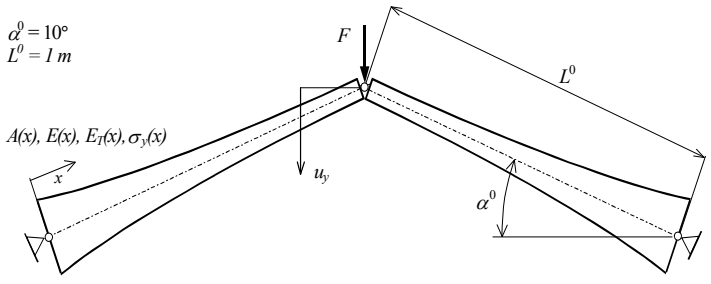

Fig. 3. Von Mises structure with varying stiffness: geometry and restrictions.

If plasticity condition in the bar is reached, it is sufficient to change the linear elastic term k_e in eq. (30) to the elastoplastic term k_{ep}

$$k_{ep} = \frac{A_i E_{Ti}}{d'_{2ep}}\left[1+\frac{3}{2}(\lambda-\lambda_{\sigma_y})L^0\frac{\overline{d'_{2ep}}}{(d'_{2ep})^2}+\frac{1}{2}(\lambda-\lambda_{\sigma_y})^2(L^0)^2\frac{\overline{\overline{d'_{2ep}}}}{(d'_{2ep})^3}\right] , \quad (35)$$

where λ_{σ_y} is the bar stretching when yield stress is reached, $d'_{2ep}, \overline{d'_{2ep}}, \overline{\overline{d'_{2ep}}}$ are the transfer constants for elastoplastic loading case. These transfer constants have a similar meaning as the transfer constants in elastic loading state, but they are callculated from second derivative of transfer function $d''_{2ep}(x) = \dfrac{1}{\eta_{AE_T}(x)}$.

The internal force before yield stress in the bar element can be calculated using formulae (32) and with the stress in the bar beyond the elastic limit, elastoplastic part of internal force can be calculated from

$$N_{iep} = -\frac{A_i E_{Ti}}{d'_{2ep}}\left[1+\frac{3}{2}(\lambda-\lambda_{\sigma_y})L^0\frac{\overline{d'_{2ep}}}{(d'_{2ep})^2}+\frac{1}{2}(\lambda-\lambda_{\sigma_y})^2(L^0)^2\frac{\overline{\overline{d'_{2ep}}}}{(d'_{2ep})^3}\right](\lambda-\lambda_{\sigma_y})L^0 \ . \tag{36}$$

Axial stress in elastoplastic domain can be calculated from

$$\sigma = \sigma_y + \frac{N_{iep}}{A_{aver}}, \tag{37}$$

where σ_y is an "average" value of the yield stress function of the bar and A_{aver} is an "average" value of the function describing the bar cross-sectional area.

In the elastic state stiffness matrix $\mathbf{K}_T(\mathbf{q})$ is expressed by (25) in the form

$$\mathbf{K}_{Te} = \frac{A_i E_{ei}}{d'_{2e}}\left[1+3(\lambda-1)L^0\frac{\overline{d'_{2e}}}{(d'_{2e})^2}+\frac{3}{2}(\lambda-1)^2(L^0)^2\frac{\overline{\overline{d'_{2e}}}}{(d'_{2e})^3}\right]\begin{bmatrix}1 & -1\\ -1 & 1\end{bmatrix}. \tag{38}$$

In the elastoplastic state it changes to form

$$\mathbf{K}_{Tep} = \frac{A_i E_{Ti}}{d'_{2ep}}\left[1+3(\lambda-\lambda_{\sigma_y})L^0\frac{\overline{d'_{2ep}}}{(d'_{2ep})^2}+\frac{3}{2}(\lambda-\lambda_{\sigma_y})^2(L^0)^2\frac{\overline{\overline{d'_{2ep}}}}{(d'_{2ep})^3}\right]\begin{bmatrix}1 & -1\\ -1 & 1\end{bmatrix}. \tag{39}$$

3. Numerical experiment – von Mises structure using trusses with varying stiffness

For examining the accuracy of the presented truss element, two numerical examples were solved. Three different types of variability of cross-sectional area and material properties were caried out. Modification of the stiffness polynomial order was considered, but ratio of maximum/minimum stiffness along the bar remained constant: $(A(x)E(x))_{\max}/(A(x)E(x))_{\min} = 2.0$ (see Fig. 5). In the first example only linear elastic material response was considered. In the second example, were carried out for bilinear elastoplastic material behaviour with isotropic as well as kinematic hardening. A typical example of the geometric nonlinear behaviour is the von Mises structure (Fig. 3). The dependence displacement vs. internal/global force for linear elastic solution of the bar with uniform cross-section is well known from literature (thin solid line in Figs. 4c and 4d). For elastoplastic behaviour this dependence is shown in this figure and comparison with the linear elastic solution is presented.

To use our new nonlinear truss element for a practical calculation a code in *MATHEMATICA* software was developed. To compare these results with the results obtained by ANSYS two different models was used:

- one dimensional model divided into 1 and 20 tapered beam elements,
- solid model meshed to 2400 brick elements grouped to 50 segments with average values of material properties in corresponding segment. The geometry of this solid model was carefully treated to approximate the variable shape of the cross-section as it was possible.

Variation of the cross-section area and material properties were considered in accordance with Tab.1.

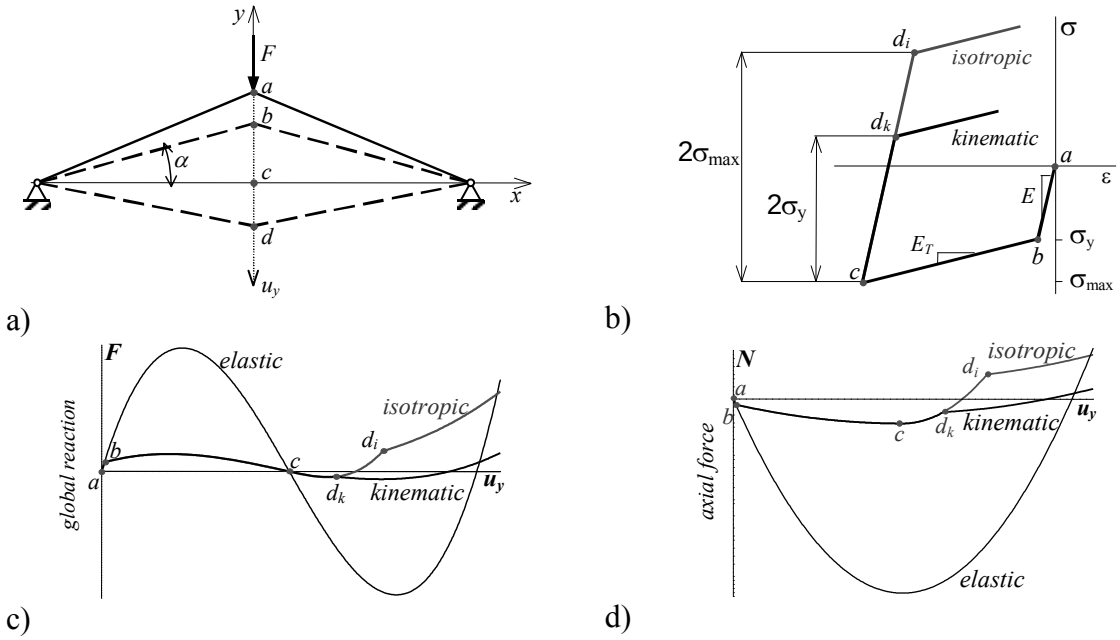

Fig. 4. Equilibrium path for linear elastic and bilinear elastoplastic material properties with isotropic and kinematic hardening of von Mises two bar structure.

stiffness function	*variation of geometry and material properties* [m^2, Pa]
AE_1	$A_1(x) = 0.0045 - 0.002x$ $E_1(x) = 2\times10^{11} - 0.2\times10^{11}x$ $E_{1T}(x) = 2\times10^{10} - 0.2\times10^{10}x$ $\sigma_{1y}(x) = 200\times10^6 - 40\times10^6x$
AE_2	$A_2(x) = 0.0045 - 0.003x + 0.001x^2$ $E_2(x) = 2\times10^{11} - 0.2\times10^{11}x$ $E_{2T}(x) = 2\times10^{10} - 0.2\times10^{10}x$ $\sigma_{2y}(x) = 200\times10^6 - 40\times10^6x$
AE_3	$A_3(x) = 0.0045 - 0.003x + 0.001x^2$ $E_3(x) = 2\times10^{11} - 0.3\times10^{11}x + 0.1\times10^{11}x^2$ $E_{3T}(x) = 2\times10^{10} - 0.3\times10^{10}x + 0.1\times10^{10}x^2$ $\sigma_{3y}(x) = 200\times10^6 - 30\times10^6x - 10\times10^6x^2$

Tab. 1. Combinations of geometric and material properties.

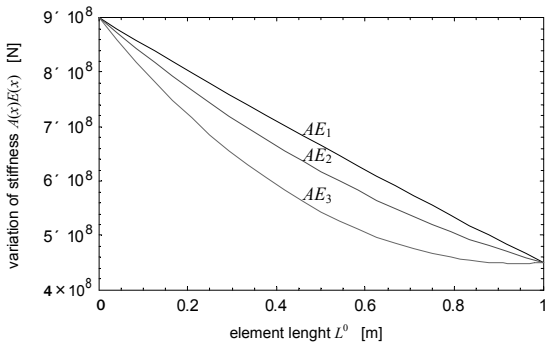

Fig. 5. Stiffness variation curves of the bar.

Example 1

In the first example our new element with ANSYS solutions were compared. In these experiments three different variations of elastic bar stiffness $B_e(x) = A(x)\,E(x)$ (Tab. 1) were used.

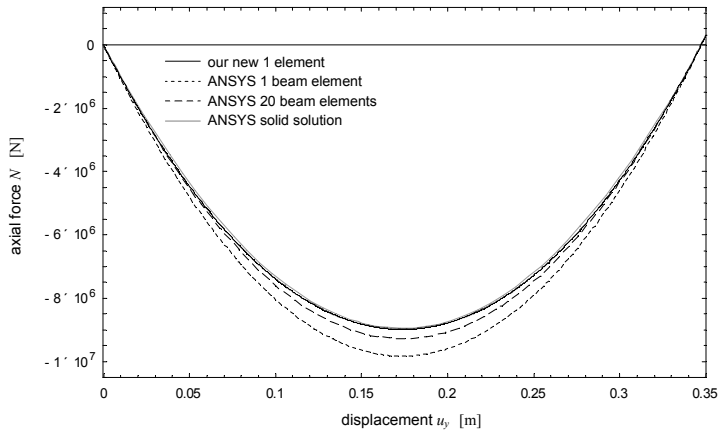

Fig. 6. Axial force – common hinge displacement response for elastic stiffness variation AE_3.

	axial force N		
	$\frac{(new\ bar\ -\ ANSYS\ 1\ beam)}{ANSYS\ 1\ beam}$	$\frac{(new\ bar\ -\ ANSYS\ 20\ beams)}{ANSYS\ 20\ beams}$	$\frac{(new\ bar\ -\ ANSYS\ solid)}{ANSYS\ solid}$
AE_1	0.91	0.26	2.27
AE_2	1.04	5.18	2.28
AE_3	0.19	5.68	1.60
	global reaction F		
	$\frac{(new\ bar\ -\ ANSYS\ 1\ beam)}{ANSYS\ 1\ beam}$	$\frac{(new\ bar\ -\ ANSYS\ 20\ beams)}{ANSYS\ 20\ beams}$	$\frac{(new\ bar\ -\ ANSYS\ solid)}{ANSYS\ solid}$
AE_1	3.77	2.37	6.04
AE_2	3.89	2.65	6.03
AE_3	2.87	3.66	5.00

Tab. 2. Absolute percentage difference between new bar analysis to ANSYS solutions [%].

Example 2

In the second example our new element with ANSYS solutions were compared. In these experiments three different variations of elastic and elastoplastic bar stiffness $B_e(x) = A(x)\,E(x)$ and $B_{ep}(x) = A(x)\,E_T(x)$ (Tab. 1) were considered.

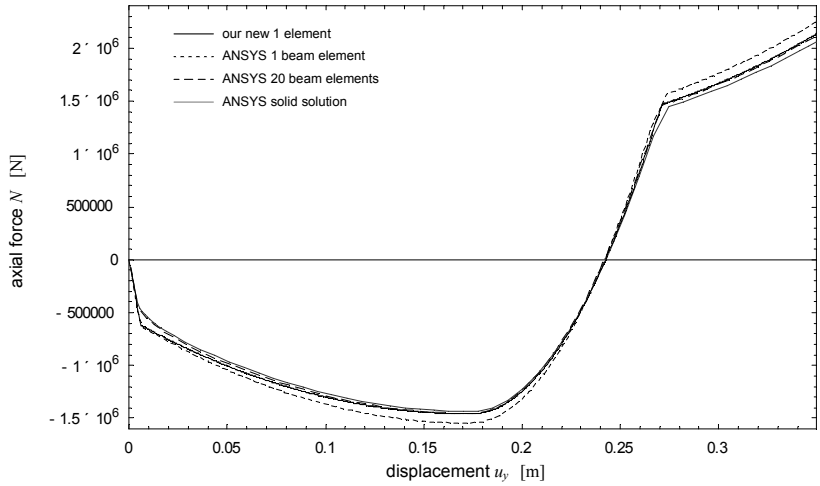

Fig. 7. Axial force – common hinge displacement response for stiffness variation AE_3 – isotropic hardening.

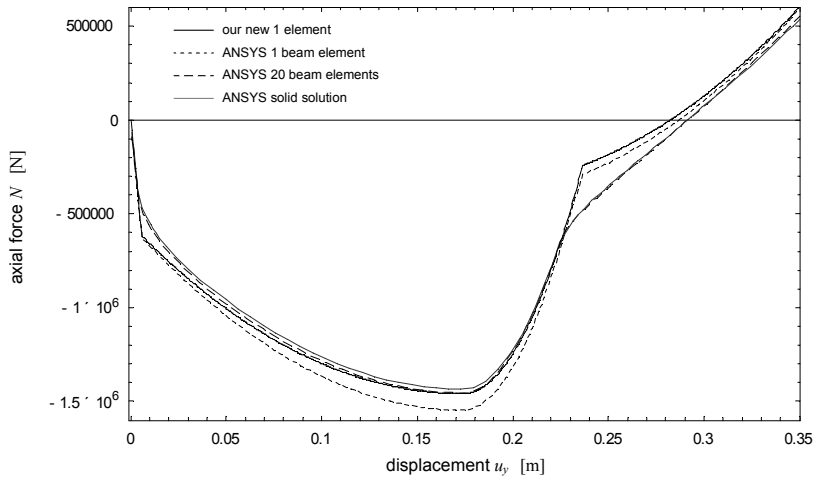

Fig. 8. Axial force – common hinge displacement response for stiffness variation AE_3 – kinematic hardening.

Resulting dependence of both the axial force N on displacement u_y at the common node are given in previous graphs. Only selected responses of axial force-displacement of common node

are presented in figures due to similarity. In Fig. 6 the of axial forces for elastic variations of stiffness AE_3 (*Example 1*) of our new truss element and ANSYS model are compared. In Tab. 2 absolute percentage differences between new bar analysis to ANSYS solutions are presented. Results obtained from numerical experiments with elastoplastic stiffness variation denoted AE_3 (*Example 2*) are shown in Figures 7 and 8. These graphs show response of internal force for bilinear material behavior. Figure 8 shows considerable differences for kinematic hardening between our solution and the ANSYS in neighbourhood of yield stress (compressive and tensile). This effect is due to fluctuating of longitudinal material properties defined in ANSYS solid model. The results of numerical analyses lead to the following conclusions:

- absolute percentage difference between the new truss element and ANSYS solution for all considered stiffness variations in elastic analysis was less then 6% for elastic loading state,
- the numerical experiments shows good agreement between the solutions of our truss element and ANSYS results by consideration of isotropic hardening, especially,
- increasing of ratio B_{max}/B_{min} influences also enlargement of differences between our new truss element and ANSYS solutions,
- considerable differences appears only for cases with kinematic hardening. This can be explained by using „average value“ σ_y to detect elastic limit in entire new truss element,
- the differences of new truss element and ANSYS models results increase with the ratio AE_{max}/AE_{min}, particularly near the yield stress,
- if stiffness ratio B_{max}/B_{min} is higher then three, results obtained with the new element are not acceptable for application in praxis and other solution have to be used for a such truss analysis.

4. Conclusion

A geometric and physically nonlinear truss finite element of composite material with continuous longitudinal stiffness variation is presented in this contribution. Continuous polynomial variation of cross-sectional area along the element has been assumed. Variation of these geometric and material parameters is described very accurate using concept of transfer functions and transfer constants.

The stiffness matrices of this finite element are derived using the full nonlinear non-incremental total Lagrangian formulation without any linearisation. The effective longitudinal material properties are calculated with the extended mixture rule. The results of numerical experiments showed high effectiveness and suitable accuracy of the new composite truss finite element. This new element fulfils the all element equations in both the global and local sense.

Acknowledgement

This work has been conducted within the grants No. 1/4122/07 and 1/2076/05 of the Slovak VEGA Grant agency. This support is gratefully acknowledged.

References

[1] V. Kutiš, Beam element with variation of cross-section, which satisfies all local and global equilibrium conditions, Ph.D. Thesis, Department of Mechanics, FEI, Slovak University of Technology, Bratislava, 2001.
[2] V. Kutiš, J. Murín, NelinPrut – an internal FEM program, Department of Mechanics, FEI, Slovak University of Technology, Bratislava, 2003.
[3] J. Murín, V. Kutiš, 3D-beam element with continuous variation of the cross-sectional area, Computers & Structures, No. 80(3-4), 2002, pp. 329-338.
[4] J. Murín, M. Aminbaghai, Vergleichsberechnungen im Rahmen der Th. II. Ordnung mit Programmen IQ-100 and ANSYS, Proceedings of Strojné inžinierstvo 99, STU Bratislava, 1999.
[5] J. Murín, V. Kutiš, Solution of non-incremental FEM equations for nonlinear continuum, Strojnícky časopis, No. 52(6), 2001, pp. 360-371.